

## **Properties of rice straw reinforced alkali activated cementitious composites**

NGUYEN, C.V. and MANGAT, Pal <<http://orcid.org/0000-0003-1736-8891>>

Available from Sheffield Hallam University Research Archive (SHURA) at:

<https://shura.shu.ac.uk/27539/>

---

This document is the Accepted Version [AM]

### **Citation:**

NGUYEN, C.V. and MANGAT, Pal (2020). Properties of rice straw reinforced alkali activated cementitious composites. *Construction and Building Materials*, 261, p. 120536. [Article]

---

### **Copyright and re-use policy**

See <http://shura.shu.ac.uk/information.html>

# Properties of rice straw reinforced alkali activated cementitious composites

Chinh Van Nguyen<sup>a,b</sup>, P.S. Mangat<sup>a\*</sup>

<sup>a</sup> Centre for Infrastructure Management, Materials and Engineering Research Institute,  
Sheffield Hallam University, Sheffield S1 1WB, UK

<sup>b</sup> Faculty of Civil Engineering, The University of Danang- University of Science and  
Technology, 54 Nguyen Luong Bang, Danang, Vietnam

\*Corresponding author: P.S. Mangat, Email address: [p.s.mangat@shu.ac.uk](mailto:p.s.mangat@shu.ac.uk); Tel:  
+44(0)1142253339

Co-authors: Chinh Van Nguyen , E-mail address: [chinhx1a@gmail.com](mailto:chinhx1a@gmail.com);  
[nvchinh@dut.udn.vn](mailto:nvchinh@dut.udn.vn); Tel: +84 (0) 9011 22 777; ORCID: 0000-0002-7953-5731

## **HIGHLIGHTS**

- Characteristics of rice straw were studied by SEMs and XRDs
- Characteristics of rice straw alkali activated cementitious composites were investigated via strengths, density, water absorption, drying shrinkage and wet/dry cycling.
- Alkali treatment enhances bond at rice straw and alkali activated cementitious paste interface
- Mechanisms of deterioration of the composites under wet/dry cycling was studied by SEMs

## Properties of rice straw reinforced alkali activated cementitious composites

### ABSTRACT

The paper investigates the characteristics of rice straw reinforced alkali activated cementitious composites (AACC). The untreated and NaOH treated rice straw at the proportion of 1%, 2%, 3% by weight of binder was added to the mixes. Characteristics of rice straw have been studied by using SEM and XRD. Mechanical properties, water absorption, drying shrinkage and durability under wet/dry cycling have been investigated to evaluate the performance of the AACCs. SEM was also used to investigate the mechanism of deterioration of the AACC. The results show that rice straw has very significant positive effects on the performance of AACCs including increase in flexural and compressive strength, durability under wet/dry cycling, large reduction in drying shrinkage, and water absorption. In addition, alkali treatment is an effective method for enhancing bond between the rice straw and the matrix leading to improved performance of AACCs.

**Keywords:** Alkali activated cementitious composite (AACC); Rice straw; Alkali treatment; Strength; Durability; Drying shrinkage; Water absorption.

## 1. Introduction

CO<sub>2</sub> emission is a key contribute to global warming and the production of Portland cement provides about 5% of global CO<sub>2</sub> emission [1]. Efforts to reduce the use of Portland cement in concrete have led to research on alkali activated cementitious materials (AACMs) in order to provide sustainable material for the construction industry. Alkali activation is the chemical reaction between a solid aluminosilicate precursor and an alkaline activator to make hardened materials. The curing temperature mainly depends on the content of calcium within the aluminosilicate. The alkali activated aluminosilicate containing high calcium content can be hardened at ambient temperature; whereas thermal treatment should be applied to induce the setting of alkali activated aluminosilicate without calcium source [2-4]. The main precursors used for producing AACMs are industrial by products such as granulated blast furnace slag derived from the steel manufacture, fly ash derived from coal combustion and natural clays (metakaolin) [5].

Characteristics of alkali activated cementitious materials have been studied by many researchers. Compressive strengths of alkali-activated, blast furnace slag high-calcium binders and fly ash-based low-calcium binders can be achieved up to 110MPa [6]. Drying shrinkage of AACMs is typically higher than that of Portland cement-based binders, when manufactured and cured under ambient temperatures, but can be controlled by good mix design of the AACM concrete [3,7] or by using shrinkage reducing admixtures [8]. The sorptivity of AACMs is within a comparable range with similar grade concretes [4]. The capillary sorptivity is reduced by employing a lower water content and a higher silica modulus activator [3]. AACM shows greater durability potential than OPC as it has lower porosity [9]. Some tests have shown that superior chloride resistance of the AACM concrete compared with a similar grade of normal Portland cement-based concrete [7]. Carbonation results of AACMs under accelerated carbonation testing often show inferior performance to Portland cement binders, which contradict data obtained under long-term natural exposure [4]. Many studies have shown better frost resistance of AACM concrete compared with similar grade conventional concretes exposed to the same conditions [10,11].

Natural fibres have been used to replace synthetic fibres to reinforce concrete or mortar for sustainable development. The natural fibres including sisal, flax, hemp, bamboo and coir are

cheaper and lighter than synthetic fibres. They are an abundant, renewable and low cost resource [12-15]. There has been far less research on cellulose fibre reinforced cement composites compared with synthetic fibres. The main drawbacks for the use of cellulose fibres as reinforcement for cement composites are the shortage of information on production techniques, failure mechanism, fibre strength, effectiveness of fibre shape and size on the performance of composites [16]. Therefore, it is necessary to conduct more research on the performance of cellulose fibre reinforced cement composites, including the effect of fibre dispersion on the matrix properties.

Rice straw is a worldwide by-product of rice production. There are some current solutions for disposal of rice straw such as livestock feeds, burning in-situ in the farm or incorporating into the soil. Each solution shows its own advantages and disadvantages. Burning at the field is considered as the cheapest method but it causes air pollution as it releases CO<sub>2</sub> [17]. The use of rice straw to provide natural fibres has been studied and rice straw shows a high potential for fibre reinforcement in cementitious mortar and concrete [17-19].

The paper investigates the characteristics of a novel alkali activated cementitious composite (AACC) for low impact buildings by incorporating rice straw fibres from agricultural waste products. The characteristics of rice straw have been determined by Scanning Electron Microscope (SEM) and X-ray powder diffraction (XRD). The performance of AACC has been investigated with a wide range of tests including compressive strength, flexural strength, water absorption, drying shrinkage and durability under wet/dry cycling. A SEM was used to study the bond at the rice straw interface with the alkali activated cementitious matrix in order to explain its influence on strength and durability of the composites material. In addition, XRD analysis was also used to determine the effect of chemical reaction between rice straw and AACM matrix on the crystalline structure of the matrix.

## 2. Experimental programme

### 2.1 Materials

The alkali activated cementitious composites consists of ground granulated blast furnace slag (GGBS) based binder, fine aggregate (sand), sodium silicate and hydroxide based activator, retarder R42 and rice straw (RS) fibres. The activator was based on a sodium silicate solution of molarity 6.5 mol/L and silica modulus 2% together with NaOH of molarity 4.8 mol/L. GGBS was supplied by Hanson Heidelberg cement Group, UK and its chemical composition is shown in Table 1. The XRD pattern of GGBS is presented in Fig. 1 which was obtained by using a Philips X-1 Pert X-ray diffractometer, operated with a Cu K $\alpha$  radiation source (40 KV and 40 mA, wavelength  $\lambda=1.5406\text{nm}$  [ $6.07 \times 10^{-9}$  2 in.]) by scanning from 5° to 75° at an angle of 2 $\theta$ , the scan step size is 0.0131303. X-ray data were fitted using the pseudo-Voigt profile function and refined by means of Rietveld. The GGBS shows a peak hump between 2 $\theta$  =20° and 40° because of the amorphous components. Fig.1 also shows that there is no significant crystalline material observed. Fine aggregate (sand) obtained from a supplier in Sheffield, UK was oven dried at 60°C for 24hours. It was sieved to remove particles retained on a 2mm size sieve then left in the laboratory air for three days before mixing and casting.

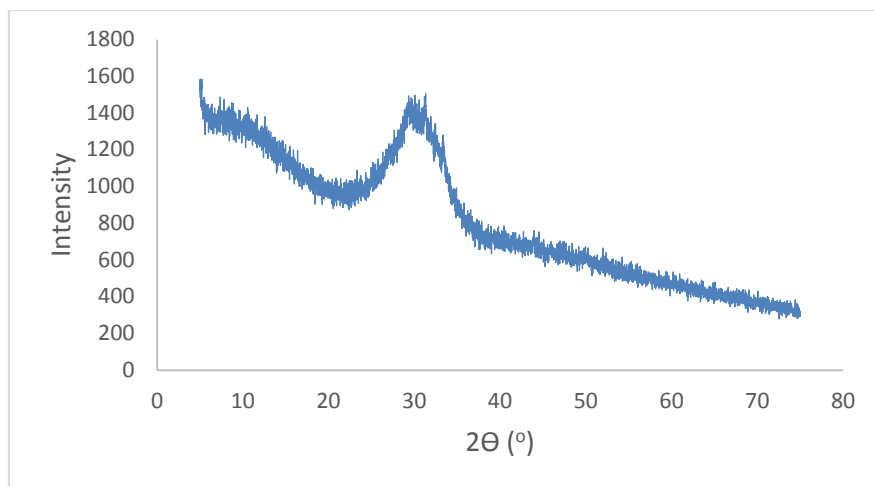


**Fig. 1. X-Ray diffractograms of GGBS**

Rice straw was received from a supplier in China. It was cut into 15-20mm lengths by using a scissors and classified as two types of fibre namely untreated rice straw (URS) and treated rice straw (TRS). For untreated fibre, the chopped rice straw was stored in an air tight bag until its use. For treated fibre, the chopped rice straw was soaked in 5%NaOH solution for 48hours in a fume cupboard, then washed with tap water until clear and oven dried at 45°C for 24 hours. The fibre was left in the laboratory air for 24hours and then sealed in an air tight bag until its use in the AACC mixes (see **Fig. 2**). This alkali treatment has proved to be effective for eliminating organic impurities and low molar mass hemicellulose thereby enhancing the fibre strength and fibre-matrix adhesion [13, 20, 21] including rice straw [18]. This treatment method also breaks down fibre bundles into thinner fibres, thereby, increasing their effective surface area [22] as can be seen in **Fig. 2. No additional physical treatment was applied to thin up the straw fibres.**



**Fig. 2. (a) Untreated and (b) treated rice straw fibres**

**Table 1**  
Chemical composition of GGBS

Constituents	GGBS
Na <sub>2</sub> O %	0.786
MgO %	11.122
Al <sub>2</sub> O <sub>3</sub> %	16.352
SiO <sub>2</sub> %	32.972
SO <sub>3</sub> %	2.109
K <sub>2</sub> O %	0.667
CaO %	34.919
TiO <sub>2</sub> %	0.24
MnO %	0.265
Fe <sub>2</sub> O <sub>3</sub> %	0.17
SrO %	0.154
BaO %	0.244

## 2.2 Details of mixes

Details of all mixes are given in **Table 2**. The mix composition of the control sample (M0) are 1: 1.94 (by weight) of binder to sand with liquid activator/binder of 0.56 and extra water/binder of 0.1. Extra water was used to improve the workability of the rice straw composites and also to compensate for the dry state of fine aggregate and fibre. The retarder R42 at ratio of 0.76% by weight of binder was added to the mix for increasing the setting time. The URS and TRS fibres were added at 1%, 2% and 3% of total binder weight, to produce composite mixes M1U, M2U, M3U and M1T, M2T, M3T respectively. The rice straw was used to replace its weight of sand in all mixes.

**Table 2**  
The mix proportions of AACC

ID	AACM Binder (%)	Sand (%)	R42 (% binder)	Liquid activator/ Binder Ratio	Water/ Binder Ratio	Rice straw	
						Amount (%Binder)	Treatment methods
M0	34	66.00	0.76	0.56	0.1	0	-
M1U	34	65.94	0.76	0.56	0.1	1	untreated
M2U	34	65.89	0.76	0.56	0.1	2	untreated
M3U	34	65.83	0.76	0.56	0.1	3	untreated
M1T	34	65.94	0.76	0.56	0.1	1	treated NaOH
M2T	34	65.89	0.76	0.56	0.1	2	treated NaOH
M3T	34	65.83	0.76	0.56	0.1	3	treated NaOH

## 2.3. Casting and curing

The AACM binder and sand were mixed for one minute and then the liquid activator was slowly added to the mix. Mixing continued for 5 min until a uniform texture was produced. The retarder admixture R42 was then slowly added while mixing continued. The rice straw fibres were gradually added to the mix together with extra water and mixing continued for 10 minutes. The same procedure was applied for the control AACM mix without adding rice

straw fibres. Specimens for all mixes were cast in 40x40x160mm and 50x50x50mm steel moulds and compacted by the vibration table in two minutes. All specimens were left in the moulds covered with polythene sheets for 24 hours in the laboratory air ( $20 \pm 2^{\circ}\text{C}$ , RH  $65 \pm 5\%$ ). After 24 hours from casting, the specimens were demoulded and cured in accordance with different test procedures as detailed in the next section.

## **2.4. Test procedures**

### *2.4.1. Rice straw characteristics*

The properties of URS and TRS fibres were determined in accordance with procedures described in [18]. SEM images of URS and TRS fibres were obtained with an ETD detector, a working distance of about 10 mm, an accelerating voltage of 5 kV and a spot size of 4 nm. XRD plots of URS and TRS fibres were obtained by using a Philips X-1 Pert X-ray diffractometer, operated with a Cu K $\alpha$  radiation source (40 KV and 40 mA, wavelength  $\lambda=1.5406\text{nm}$  [ $6.07 \times 10^{-9}$  2 in.]) by scanning from  $5^{\circ}$  to  $75^{\circ}$  at an angle of  $2\theta$ , the scan step size is 0.0131303. X-ray data were fitted using the pseudo-Voigt profile function and refined by means of Rietveld.

### *2.4.2. Consistency of fresh composites*

The workability of fresh mortar was measured with the flow table test in accordance with BS EN 1015-3:1999 [23]. The flow value represented the mean diameter of a test sample of the fresh mortar placed on the flow table disc by means of a defined mould and given a number of vertical impacts by raising the flow table and allowing it to fall freely through a given height.

### *2.4.3. Dry bulk density*

Dry bulk densities of hardened mortar were determined in accordance with BS EN 1015-10:1999 [24]. Three cubes of 50x50x50mm were cast and cured in water. At 28 days age, the cubes were oven dried at  $60^{\circ}\text{C}$  for 48 hours to reach the constant mass for calculation of the dry bulk density.

### *2.4.4. Mechanical properties*

The flexural and compressive strengths were determined in accordance with BS EN 196-1:2005 [25]. After demoulding, three prisms of 40x40x160mm dimensions were used to determine the flexural and compressive strength at 1 day age while another 6 prisms were cured in water in the humidity room ( $20^{\circ}\text{C}$ , RH45%) to determine strengths at 14 and 28 days age. The three point bending test method was used to determine the flexural strengths. The two halves of the broken prisms from the flexural strength tests were used to determine the compressive strengths. Hence, the strength measurements of AACC were made at 1, 14 and 28 days age. Each result of the flexural and compressive strength was the average value of three and six specimens respectively.

SEM (QUANTA 650) was also used to observe the bond at the straw matrix interface. Samples for SEM were taken from the 28 day age specimens, oven dried for 4 hours before coating with a 20 nm thick layer of gold using a Quorum Q150T. SEM images were obtained with an ETD detector, a working distance of about 10 mm, an accelerating voltage of 5 kV and a spot size of 4 nm.



XRD was used to study the effect of the treatment method of the rice straw on the mineralogical compositions of alkali activated cementitious matrix at 28 days by testing samples of M0, M2U, M2T. AACM matrix from broken flexural strength test samples, after removing of the rice straw, was crushed by the hammer and powder was sieved under 7.5  $\mu\text{m}$  for XRD test samples. XRDs were conducted on a Philips X-1 Pert X-ray diffractometer. They were operated with a Cu K $\alpha$  radiation source (40 KV and 40 mA, wavelength  $\lambda=1.5406\text{nm}$  [ $6.07 \times 10^{-9}$  2 in.]) by scanning from 5° to 75° at an angle of 2 $\Theta$ , the scan step size is 0.0131303. X-ray data were fitted using the pseudo-Voigt profile function and refined by means of Rietveld Refinement

#### 2.4.5. Water absorption test

Test was conducted in accordance with ASTM C1403-15: Standard test method for rate of water absorption of masonry mortars [26]. Three cubes of dimensions of 50x50x50mm were cast and demoulded after 24 hours. After demoulding, they were put in an air tight plastic bag and cured in a desiccator for 28 days before performing the water absorption test.

#### 2.4.6. Drying shrinkage

The drying shrinkages of the different compositions of AACC were determined according to ASTM C596 -18: Standard test method for drying shrinkage of mortar containing hydraulic cement [27]. Three prism specimens of 160mm length and 40x40 mm cross section were cast and demoulded after 24 hours. Two demec points were attached on each face of the prism at a gauge length of 100 mm to measure the distance (strain) between them with an extensometer. The samples were then cured in water at 20°C. They were removed from water at 3 days after casting, dried with a cloth and the first (datum) strain reading was taken with a demec extensometer. The shrinkage specimens were then cured in the humidity room at 20°C, 45% RH. Subsequent shrinkage readings were taken at regular intervals up to 90 days with the extensometer.

#### 2.4.7. Durability under wet/dry cycling

Wet/dry cycling tests were performed on six prisms of dimensions 40x40x160mm for each mix. They were demould 24 hours after casting and cured in water until 28 days age. Three prisms (set A, reference) were continuously cured in water until the test date. An other three samples (set B) were subjected to wet/dry cycles. Each cycle consisted of 24 hours in water at 20°C and 24 hours in the oven (60°C). The specimens were dried to attain a surface dry condition before being placed in the oven, and they were also allowed to cool to room temperature before being immersed in the water. Therefore, one cycle consisted of 23.5 hours wet at 20°C, 0.5 hour lab air (20°C, 65%RH), 23.5 hours dry (oven, 60°C, 20%RH) and 0.5 hour lab air (20°C, 65%RH). At 71 days age (20 wet/dry cycles), all wet/dry curing samples (set B) and water curing samples (set A) were tested to determine the flexural and compressive strengths. The retained strength ratio is defined as the ratio of strength of the samples after 20 wet/dry cycles curing (set B) to strength of the samples cured in water at 20°C, 45%RH for the duration of the durability test (set A, reference). SEM tests were also conducted to determine the reason for strength loss such as bond loss at the rice straw fibre/cement matrix interface or damage/strength loss of rice straw fibre or cracking of the alkali activated cementitious matrix.



## 3 Results and Discussion

### 3.1. Characteristics of rice straw

#### 3.1.1. SEM study

SEM images of URS and TRS fibres are shown in **Fig. 3**. The surface of URS fibre is quite regular and covered with a layer of substance which includes oils, waxes and extractives such as lipids, phenolic compounds, terpenoids, fatty acids, resin acids, etc..[18]. The surface of TRS fibre is rough as the NaOH treatment removes extractives, waxes, oil and amorphous constituents such as hemicellulose and lignin from fibre surfaces [28]. **It can be seen that the surface of TRS fibres has greater roughness than the URS fibres thus promising greater bond strength with the matrix.**

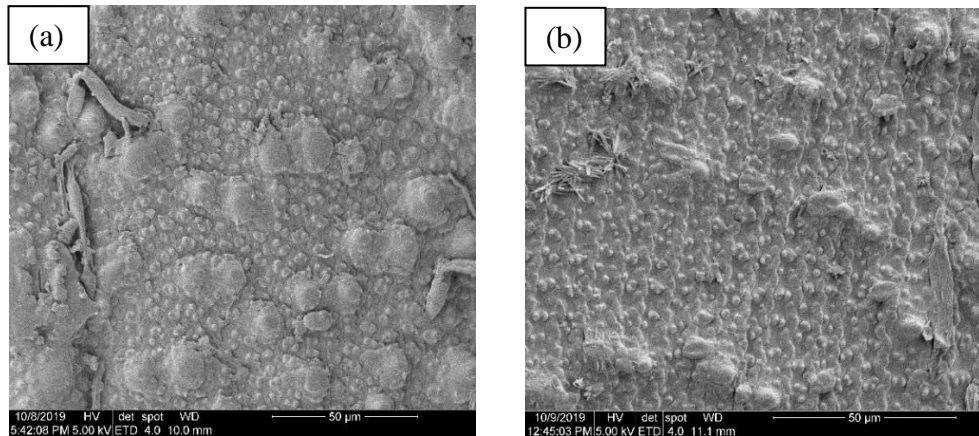


**Fig. 3.** SEM micrographics of (a) URS and (b) TRS

#### 3.1.2 XRD study

XRD plots of URS and TRS fibres are presented in **Fig. 4**. There are only two clear peaks appearing at around  $2\theta=18^\circ$  and  $22^\circ$  for both URS and TRS fibres and the spectrums are very similar for both type of fibres. However, it is clear that the peaks of TRS are slightly higher than that of URS fibres due to the removal of the amorphous materials which agree well with previous research [18]. The degree of crystalline Cellulose (I) in the total cellulose can be expressed by the X-ray “crystallinity index CI” as follows [18, 29, 30] using the data in **Fig. 4**. The results are presented in **Table 3**.

$$CI = 100 \times \frac{I_{002} - I_{am}}{I_{002}}$$

In which:  $I_{002}$  is the intensity of the principal cellulose (I) peak at  $2\theta=22^\circ$   
 $I_{am}$  is the intensity due to the amorphous part of the sample at  $2\theta=18^\circ$ .

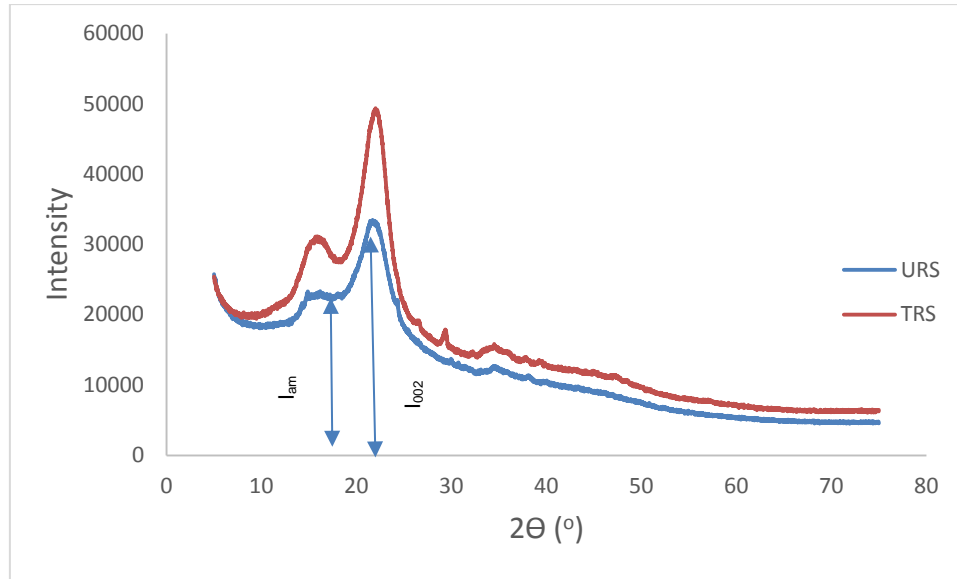


**Fig. 4.** X-Ray diffractograms of treated and untreated Rice straw

**Table 3**

Degree of crystalline cellulose of untreated and treated rice straw

Fibres	$I_{002}$	$I_{am}$	CI (%)
Untreated rice straw (URS)	33463	22509	32.7
NaOH treated rice straw (TRS)	49372	27448	44.4

**Table 3** shows that crystallinity index of TRS fibres is about 35% (from 32.7% for URS to 44.4% for TRS) higher than the URS fibres which is due to the part of the amorphous materials. This result also agrees well with the previous research conducted on rice straw sources from Egypt [18].

### 3.2. Workability

The flows of all mixes are given in **Fig. 5**. The rice straw fibres reduced the flow of the AACC and the workability (flows) decreased with increasing volume of rice straw fibres. The reduction in workability of rice straw composites can be due to water absorption by the hydrophilic natural fibres. The loss of workability of natural fibre composites depends mainly on the fibre aspect ratio and volume fraction in the mixtures [16]. Previous research shows that the increase in length and content of jute fibre resulted in the decrease in workability [31]. It is also reported that the workability of cement composites reduced when eucalyptus pulp, coir or eucalyptus pulp combined with sisal fibres [32] were added to the matrix.

**Fig. 5** also shows that the TRS fibres resulted in a higher reduction in workability than the URS fibres. This can be explained by the increase in dry surface areas of TRS fibres compared with the URS fibres (see **Fig. 2**). For improvement of workability of rice straw composites, the straw fibre can be pre-wetted before adding to the mixtures, or by consideration of the water absorption property of fibres in the mixture design [16] or using superplasticizer.

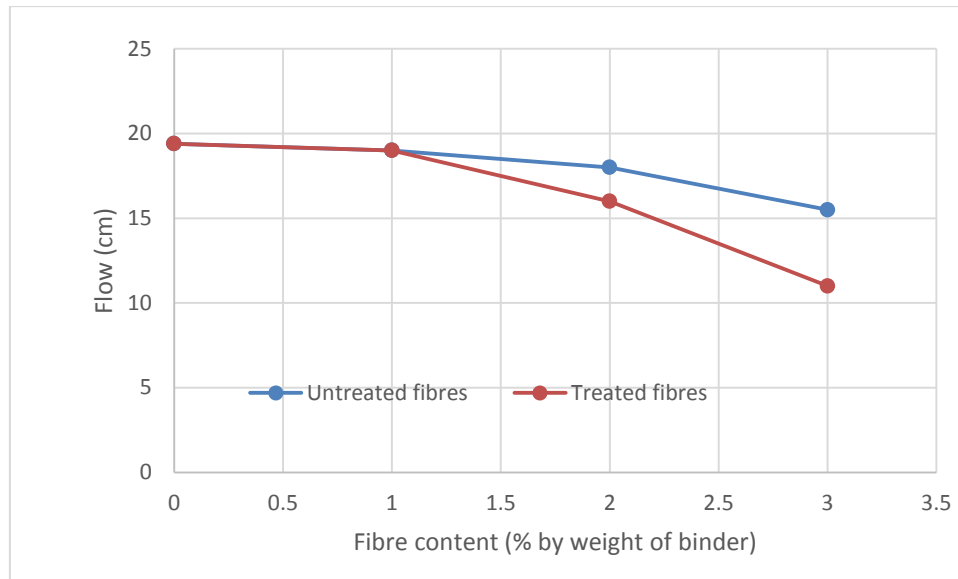


**Fig. 5.** Flow of fresh rice straw composites

### 3.3. Dry bulk density

The dry bulk density of all composites is given in **Fig. 6**. It can be seen that 2% and 3% addition of URS reduced the density of the ACCC while there is a slight increase of density when 1% of URS is added. The alkali treated rice straw increases the density of alkali activated cementitious composites when added at the proportion of 1% and 2% by weight of binder but reduced the density of the composite when added at 3% compared with the control sample M0. This agrees well with the water absorption test results in section 3.5. Within the range of 1-3% fibre content, the density decreases with increasing rice straw fibre content for both untreated and treated fibres. The largest difference of the density between URS and TRS fibres are at 3% fibre content which is only more than 5% (from 1.727 g/cm<sup>3</sup> for M3U to 1.818 g/cm<sup>3</sup> for M3T). It shows that the difference between density of URS and TRS composites is not significant.

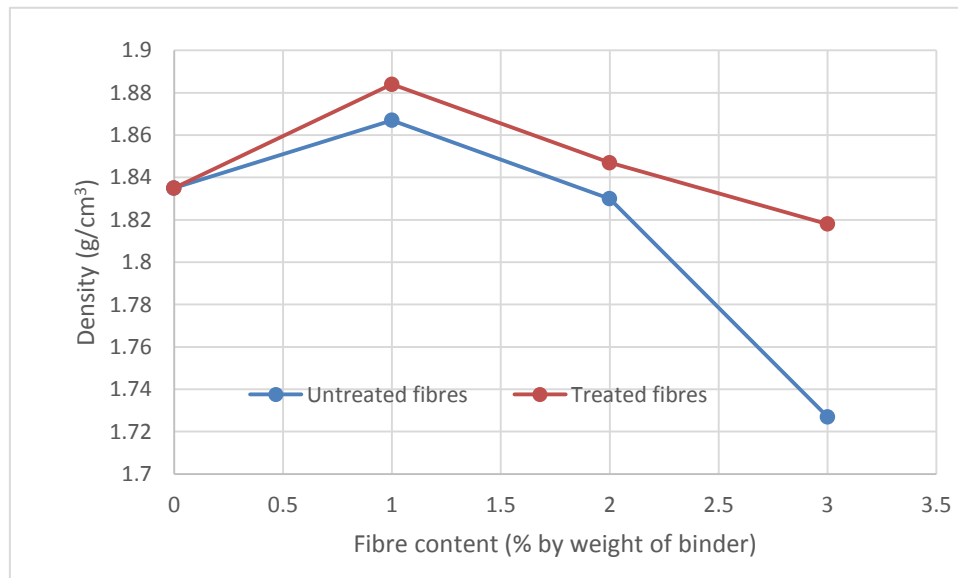


**Fig. 6.** Dry bulk density of hardened rice straw composites

## 3.4 Mechanical properties

### 3.4.1 Flexural strength

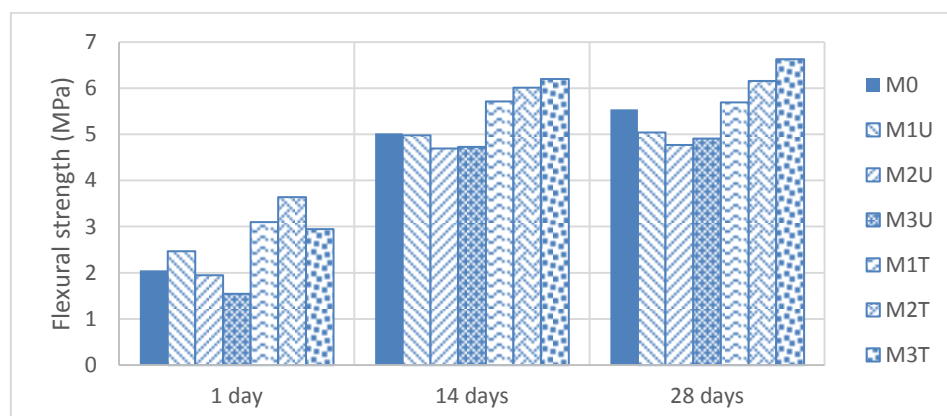


**Fig. 7.** Flexural strengths of AACCs

The flexural strengths of all AACCs are plotted in **Fig. 7**. It is clear that the URS reduced the flexural strength while the NaOH TRS increases the flexural strength compared with the control sample without rice straw at 1 day, 14 days and 28 days, except for the increase in flexural strength indicated at 1 day with the 1% of URS fibre reinforced composite. The largest reductions up to 6.5% in flexural strength are at 2% of URS reinforcement (from 5.02MPa for M0 to 4.69MPa for M2U) at 14 days and 13.8% (from 5.54MPa for M0 to 4.77MPa for M2U) at 28 days. In contrast, the TRS increases the flexural strength of alkali activated cementitious composites. It also been seen that at early age (1 day) the largest increase in flexural strength is at 2% TRS fibres, however, at later age (14 and 28 days), it is at 3% TRS. This can be explained by the aging effect on the bond of TRS fibre with the matrix. Aging effect on bond has been investigated by many researchers where the bond strength at steel fibre/ cement matrix interface rapidly increased with age [33, 34]. The frictional bond strength of polyethylene (PE) fibre in plain and silica fume matrices under moisture curing increased from 0.5 to 28 days age [35]. The increase in bond strength with age is due to the increase in strength of matrix surrounding the fibres [33, 36-39]. This can also be applied to the cellulose fibres as the increase in bond at rice straw fibre interface is due to the increase in strength of the matrix surrounding the rice straw. Therefore, at 14 and 28 days age, increasing percentage of TRS results in the higher increase in flexural strength. The increases in flexural strength of 3% TRS fibre composites compared with the control sample are 23.5% (from 5.02MPa for M0 to 6.20MPa for the M3T) at 14 days and 19.7% (from 5.54MPa for M0 to 6.63MPa for M3T) at 28 days. It is also noted that the rice straw fibres fractured under flexural testing in both URS and TRS samples (see **Fig. 8**) proving that the bond strength of the rice straw fibres with the matrix was higher than the tensile strength of rice straw fibres.

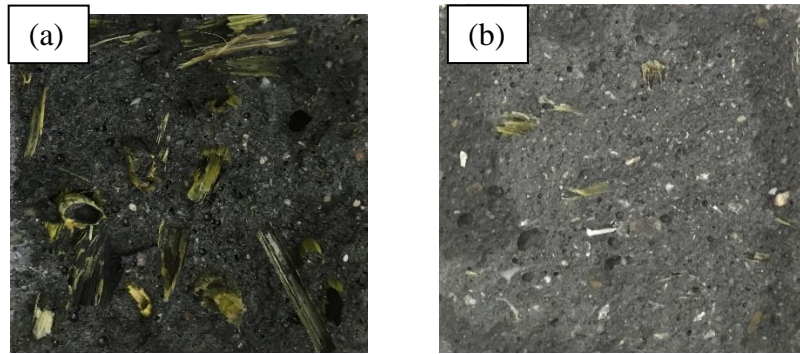


**Fig. 8.** Failures of a) URS and b) TRS fibres under flexural testing

### 3.4.2. Compressive strength

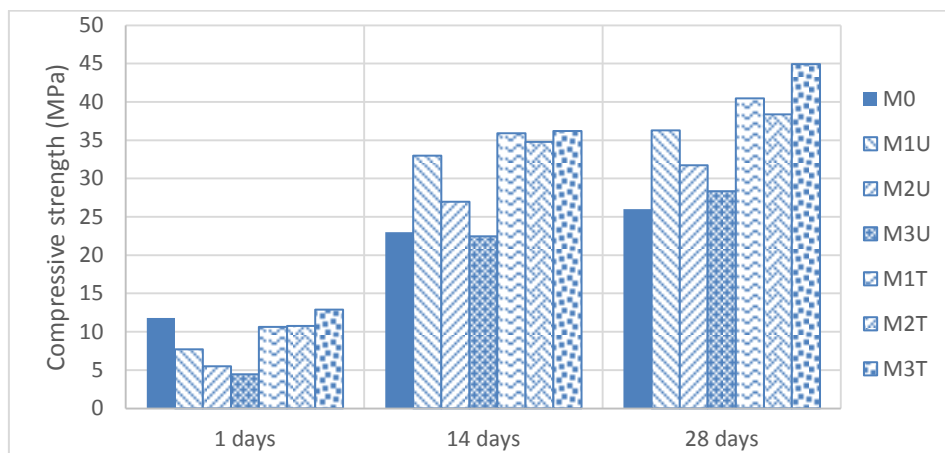


**Fig. 9.** Compressive strength of alkali activated cementitious composites

The compressive strengths of AACCs are shown in **Fig. 9**. The compressive strength of composites reduced at early age (1 day) when URS fibres were added to the AACM mortar, the strength decreased with increasing of fibre content. However at 14 days, 1% and 2% URS increase the compressive strength while 3% URS composite has similar strength to the control samples (M0). At 28 days, all 1%, 2% and 3% URS composites have higher compressive strengths than the control sample M0. The increase in compressive strength of URS composites compared with the control sample at 14, 28 days can again be explained by the aging effect detailed in section 3.4.1 as the increase in the strength of matrix surrounding the fibres. The optimum proportion of URS is 1% within the range of investigation with the increase in compressive strength of nearly 40% (from 26.0 MPa for the control sample M0 to 36.29MPa for the M1U) at 28 days.

In contrast to the URS, the TRS fibres generally improve the compressive strength of the composite. At early age (1 day), 1% and 2% TRS slightly reduced the compressive strength while 3% TRS improved the compressive strength. At 14 days and 28 days, the TRS improved significantly the compressive strengths which increase with increasing straw content. The better performance of TRS fibre composite compared with the URS can be explained by the improvement of bond at the interface with the matrix due to the increase in effective surface area [22] and surface roughness as explained in detail in the next section.

The maximum increase in compressive strength is at 3% TRS composite which are around 57% (from 23.0MPa for M0 to 36.19MPa for M3T) at 7 days and 73% (from 26.0MPa for M0 to 44.93MPa for M3T) at 28 days. This is not in line with the density results in section 3.3 as 3% of both URS and TRS reduces significantly the density of the composites. The reason is that the compressive strength is less affected by fibre density and also improved by the hydrophilic nature of the fibres helps.

The compressive strength of the AAC composites is primarily controlled by the AACM matrix strength. Therefore, the increase in compressive strength of AACCs compared to the control can be explained by the hydrophilic nature of rice straw fibres which leads to a reduction in liquid activator/ binder ratio of the matrix compared to the control. In addition, the liquid activator absorbed in the rice straw fibres also works as the internal curing agent of the cementitious matrix enhancing its strength. While the URS absorbed less liquid activator than the TRS then this hydrophilic effect shows more effectiveness in TRS composites than URS composites. This is similar to the effect of porous lightweight aggregates in concrete [39].

### 3.4.3 Scanning Electron Microscope Study

Bond at the fibre- matrix interface is an important factor effecting the strength of the composite as the stress can be transferred from the cement matrix to the fibres throughout the interface under loading [40, 41]. One of the drawbacks of using natural fibres in cementitious composites is the poor bond due to the hydrophilic nature of natural fibre. The bond failure at fibre and cement matrix interface under loading is due to poor chemical and physical interfacial interaction between natural fibre and cement matrix [42]. The chemical treatment with NaOH solution was used to eliminate lignin, natural fats, waxes and impurities from the fibre surface to improve the surface roughness of natural fibres [43, 44] and surface modification for enhancing the interfacial interaction [45]. The SEM images in **Fig. 10** show that rice straw, after alkali treatment, improved the interfacial interaction since the gap (crack) between the matrix and TRS interface (**Fig. 10b**) is quite small compared with the URS (**Fig. 10a**). In the case of TRS (**Fig.10b**) the matrix appears to have merged with the fibre at the interface. It can also be seen that surface roughness of rice straw is improved significantly after alkali treatment enhancing the bond strength (**Fig. 3**).

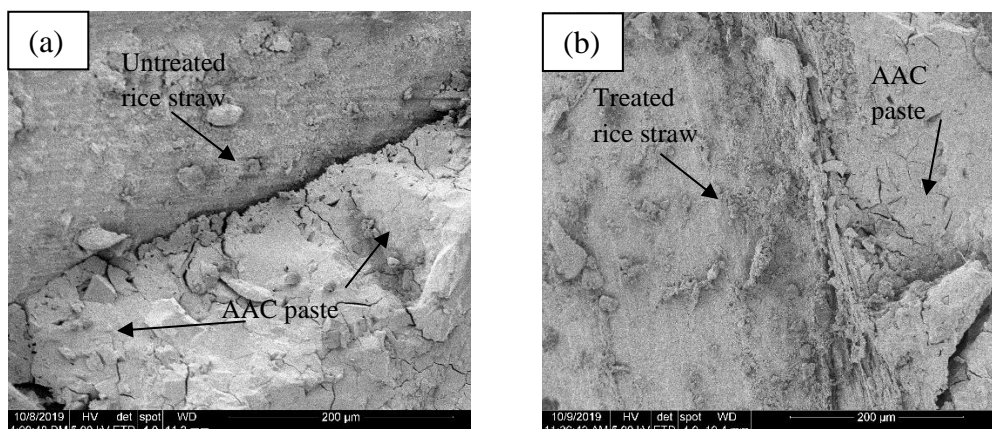


**Fig.10.** SEM images at (a) URS fibre- matrix interface and (b) TRS fibre- matrix interface

### 3.4.4. XRD Analysis



Mineralogical compositions of alkali activated cementitious paste at 28 days of M0, M2U, M2T are shown in **Fig. 11**. It can be seen that the XRD patterns of the three composites are very similar showing presence of quartz, calcite and gypsum. The peaks of quartz at  $2\theta=27^\circ$  increased slightly as rice straw was used in the composite and the peak of quartz of TRS composite is significantly higher than that of URS composite. The total  $\text{CaCO}_3$  reduced slightly when rice straw was added to the mixes with TRS reducing  $\text{CaCO}_3$  more than the URS. The rice straw and its treatment methods have slight influence on the mineralogical compositions of alkali activated cementitious paste. This may due to the impurity of rice straw surface and the NaOH solution used for rice straw treatment.

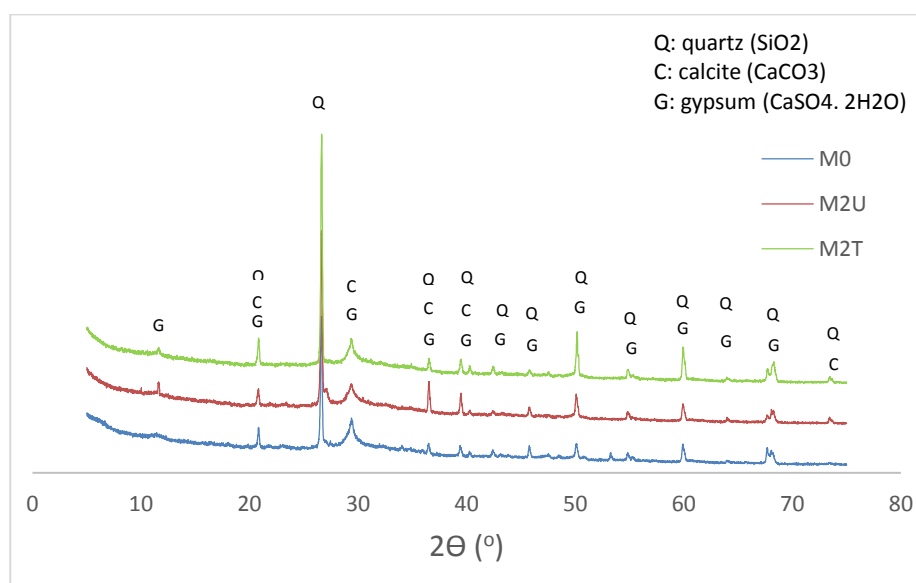


**Fig. 11.** X-ray diffraction patterns of AACM powder taken from the control (M0); URS composite (M2U) and TRS composite (M2T) at 28 days age

### 3.5. Water absorption

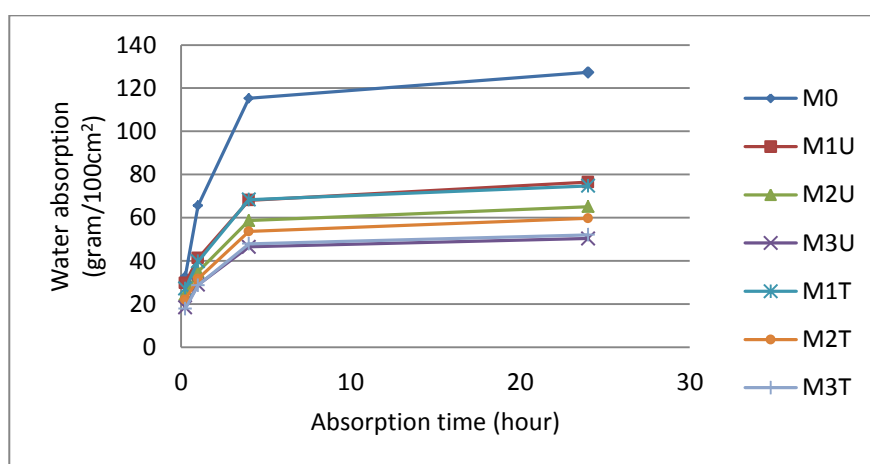


**Fig. 12.** Water absorption of alkali activated cementitious composites

**Fig. 12** shows that both URS and TRS reinforcement improves the water resistance of the composites. The water absorption of 1% and 3 % of both URS and TRS composites are very similar while the water absorption of 2% URS composite is slightly higher than that of TRS



composite. The graph also shows that increasing straw content reduces the water absorption. This agrees well with the previous research where a collated cellulose fibre at volume fractions of up to 0.5% was used in concrete and contributed to the reduction in the permeability of concrete [46]. The reduction in water absorption of fibre composites may due to the reduction in bleeding as fibres increase mix stiffness and reduce the settlement of aggregates (sand). This is also not in line with the results of the density in section 3.3 as the water absorption of the composites is less affected by fibre density, but improved by the hydrophilic nature of the fibres. Rice straw fibres absorb more liquid in the mix thereby reducing the liquid activator/binder ratio and providing the liquid as an internal curing agent. This contributes to enhanced quality of the AACM matrix (greater strength and lower porosity), thus leading to a reduction in the water absorption. The largest reduction in water absorption is up to 60% when 3% URS was added to the alkali activated cementitious mortar.

### 3.6 Drying shrinkage

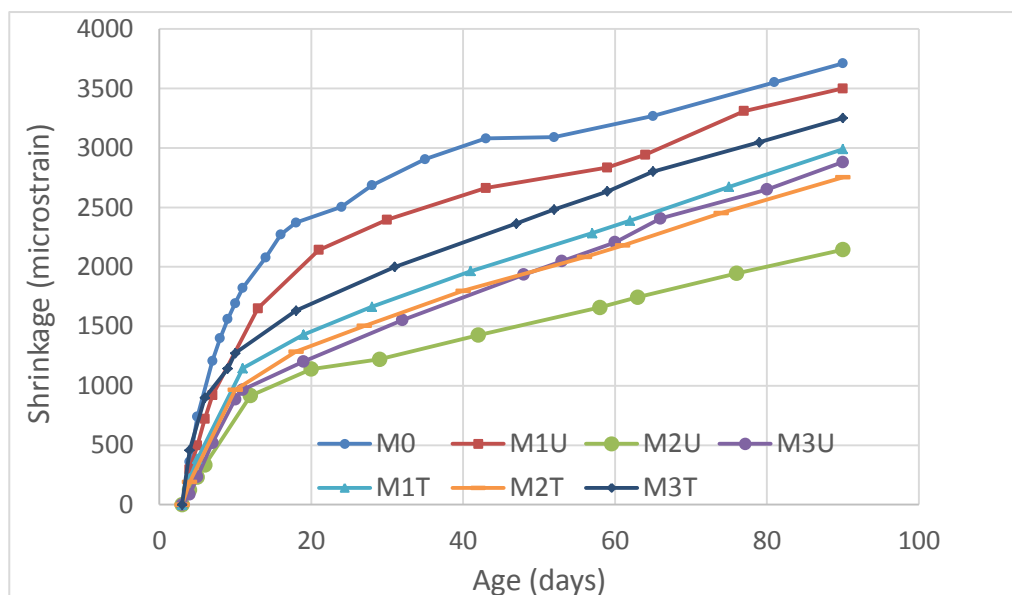


**Fig. 13.** Shrinkage of the alkali activated cementitious composites

The shrinkages of rice straw fibre AACCs (2% and 3% URS and TRS) and the control mortar up to 90 days are shown in **Fig. 13**. It is clear that both URS and TRS contributed to the reduction in drying shrinkage of the AACM mortar. It is known that the drying shrinkage is due to the evaporation of free water. **Apart from 1% rice straw fibres, the drying shrinkage of URS composites is less than the TRS composites and the optimum occurs at 2% URS.** At 90 days the 2% URS composite (M2U) had a drying shrinkage of about 40% of the control sample (M0) This may be due to the reduction in pore volume of alkali activated cementitious composites as the rice straw was added. This is confirmed by the results of water absorption tests in section 3.4 where rice straw reduces water absorption of alkali activated cementitious composites. The reduction in drying shrinkage of rice straw composites compared to the control can also be explained by the hydrophilic effect of the straw. Rice straw absorbed the liquid and reduced the liquid activator/ binder ratio while providing internal curing enhancing the impermeability of the matrix. This leads to the reduction in drying shrinkage by reducing moisture loss from the matrix.

Synthetic fibres such as carbon, steel, glass have a positive effect on the drying shrinkage of cementitious mortar [47-49] while some natural plant based fibres have a negative effect on the drying shrinkage of cementitious composites [50, 51]. Previous research shows that the drying shrinkage decreases by the addition of carbon fibres depending also on the treatment of carbon fibre; it decreased by up to 32% when 0.5% of silane-treated carbon fibres, by weight of cement, were added [47]. Steel fibre also reduced shrinkage by 40% to 83% when 1-3% of fibres by volume were added [48, 49]. Previous research shows that the effect of other plant based natural fibres on the drying shrinkage of cementitious mortar depends on the fibre characteristics and fibre content leading to the effect on matrix pore structures [50]. Short sisal and coconut fibres at 2-3% volume increased drying shrinkage. The higher drying shrinkage of composites containing sisal fibre is attributed to the higher water absorption and less smooth surface of sisal fibre compared with coconut fibre [50]. Other research also reported that sisal fibre increases drying shrinkage due to the increased porosity of samples containing sisal fibre [51]. Therefore, rice straw fibre has positive effect on the reduction in drying shrinkage than other natural plant based fibres. Rice straw composite reduced drying shrinkage by up to 40% at 90 days compared with the control sample without rice straw fibres. The drying shrinkage of the rice straw fibre composites also depends on the content and treatment methods of fibres.

### 3.7. Durability under wet and dry cycling

#### 3.7.1. Effect of wet dry cycling on the compressive strength

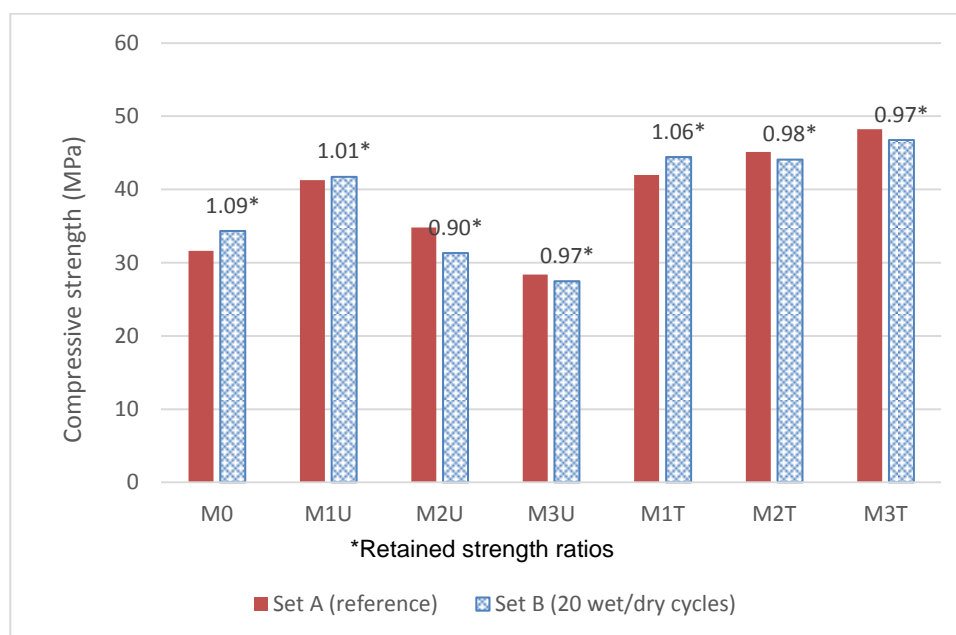


**Fig. 14.** Compressive strength of AACC under wet/dry cycling

The compressive strengths of AACCs (M1U, M2U, M3U, M1T, M2T, M3T) and control sample (M0) of set A (reference) which were cured in water and set B (20 wet/dry cycles) are presented in Fig. 14. The retained compressive strength ratios defined as the ratio of compressive strength of the set B (20 wet/dry cycles) samples to compressive strength of the set A (reference) samples for the duration of the durability test are also presented in Fig. 14. The composites with 1% URS and 1%, 2% and 3% TRS showed an increase in the compressive strength under 20 wet/dry cycles curing compared with the control sample (M0).

The compressive strength of the control sample without rice straw (M0) after 20 wet/dry cycles curing is 34.31MPa while the compressive strength of 1%, 2% and 3% URS reinforced composites after 20 wet/dry cycles curing are 41.71MPa, 31.32MPa, and 27.45 MPa respectively; the compressive strength of composites reinforced with 1%, 2% and 3% TRS after 20 wet/dry cycles curing are 44.44MPa, 44.09MPa and 46.73 MPa respectively. The 3% TRS is the optimum composite for compressive strength under wet/dry cycling.

### 3.7.2 Effect of wet dry cycling on flexural strength

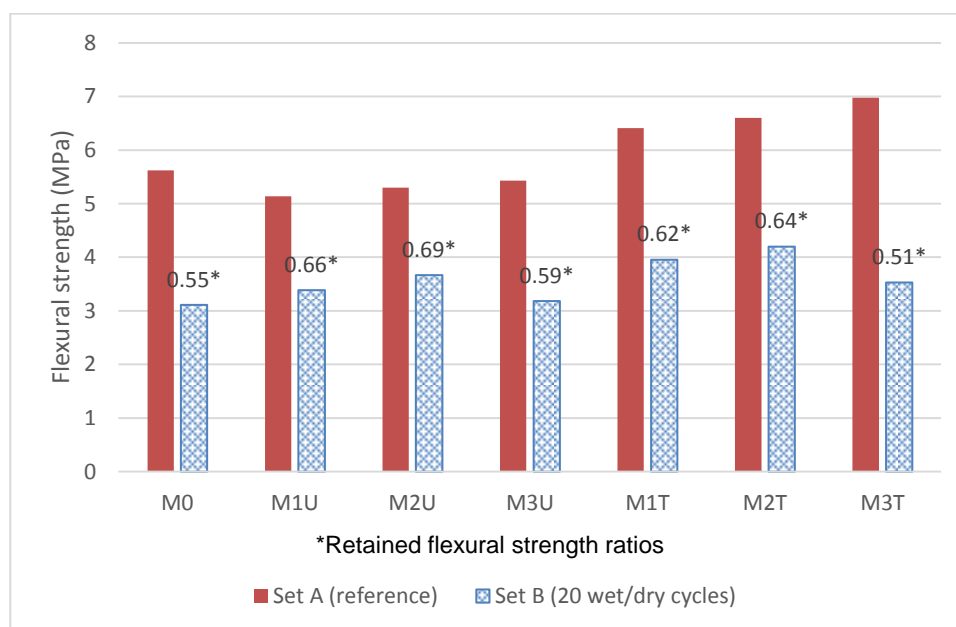


**Fig. 15.** Flexural strength of AACCs under wet/dry cycling

The flexural strengths of AACC and the control samples without rice straw fibres (M0) of set A (reference) which were cured in water and set B (20 wet/dry cycles) are presented in **Fig. 15**. The retained flexural strength ratios defined as the ratio of flexural strength of the set B (20 wet/dry cycles) samples to flexural strength of the set A samples (which were cured in water) for the duration of the durability test are also presented in **Fig. 15**. Both URS and TRS reinforcement increased the flexural strengths of composites after 20 wet/dry cycles curing compared with the control samples without fibres (M0). The flexural strength after 20 wet/dry cycles curing of the control sample without fibres (M0) is 3.11MPa compared with 3.39MPa, 3.67MPa and 3.18 MPa for 1%, 2%, and 3% URS fibre reinforcement respectively. The flexural strengths of 1%, 2% and 3% TRS composites after 20 wet/dry cycles curing are 3.96MPa, 4.2MPa and 3.53MPa respectively.

The retained flexural strength **ratio** of control sample (M0) is 0.55 while the retained flexural strengths **ratios** of 1%, 2% and 3% URS composites are 0.66, 0.69 and 0.59 respectively; the retained flexural strength **ratios** of 1%, 2% and 3% TRS composites are 0.62, 0.64 and 0.51 respectively. There were reductions in flexural strength after **20 wet/dry cycles** for both the AACCs and control samples (M0).

The failure of all specimens under flexure occurred with the fracture of straw fibre under 20 wet/dry cycles (Fig. 16). Although under 20 wet/dry cycles there was visual evidence of bond defect of the straw- matrix interface the residual strength was still larger than the strength of the fibres.



**Fig. 16.** Failures of treated rice straw after 20 wet/dry cycles under flexural testing

Fig. 14 shows that the compressive strength of set A (references) which were cured in water and set B (wet/dry cycles) of all AACCs and the control mix are similar, with the retained strength ratios between 0.9 and 1.09, with most values falling between 0.97 and 1.06. This indicates that the 20 wet/dry cycles exposure does not cause any significant reduction in compressive strength. Since the compressive strength of the AAC composites is primarily controlled by the AACM matrix strength with the rice straw fibres contributing primarily to flexural strength and crack control, this indicates that the wet/dry cycles have not affected the durability of the composites with respect to compressive strength. The flexural strengths of the composites and the control mix M0, however, show a substantial reduction relative to the set A (references) which were cured in water (see Fig. 15). The causes of this reduction are shown in the SEM photos given in Fig. 17. Fig. 17b shows greater micro cracking in the matrix of AACCs subjected to 20 wet/dry cycles compared to the continuously wet cured specimens (set A) due to the high temperature curing cycle at 60deg C in the former case. This micro cracking has reduced the flexural strength but the compressive strength has not been similarly affected as it is less sensitive to this micro cracking. The contribution to flexural strength reduction by interfacial bond loss of URS fibres after 20 wet/dry cycles' exposure relative to set A (reference) which were cured in water is shown in Figs. 17c and 17d where a significant gap between the fibre interface and the matrix can be observed. However, Figs. 17e and 17f show that the bond between the TRS fibres and the AACM matrix remains relatively intact under both wet/dry exposure and water curing only (set A) but the fibre shows a degree of longitudinal cracking (Fig. 17f) due to the 60 deg C drying cycle.

### 3.7.3. Mechanisms of deterioration under wet/dry cycling

Previous research on kraft pulp fibre–cement composites showed that under wet /dry cycling, composite failure is due to the initial fibre–cement debonding due to fibre shrinkage during drying, reprecipitation of relatively low-strength hydration products within the new void space produced at fibre–cement interface and fibre mineralization by the re-precipitation of hydration products, likely calcium hydroxide [52]. The failure mechanisms of rice straw fibre



and cementitious matrix under wet/dry cycles can be also proposed as follows: i) initial bond failure under dry cycles as fibre shrinks during drying at high temperature; ii) new AACM products filling the void space caused by rice straw shrinkage and protecting the rice straw fibre during wet cycles iii) rice straw mineralization by the AACM products, leading to embrittlement of rice straw fibres, iv) Micro-cracks appearing in the AACM matrix under the 60°C drying cycle and reducing flexural strength.

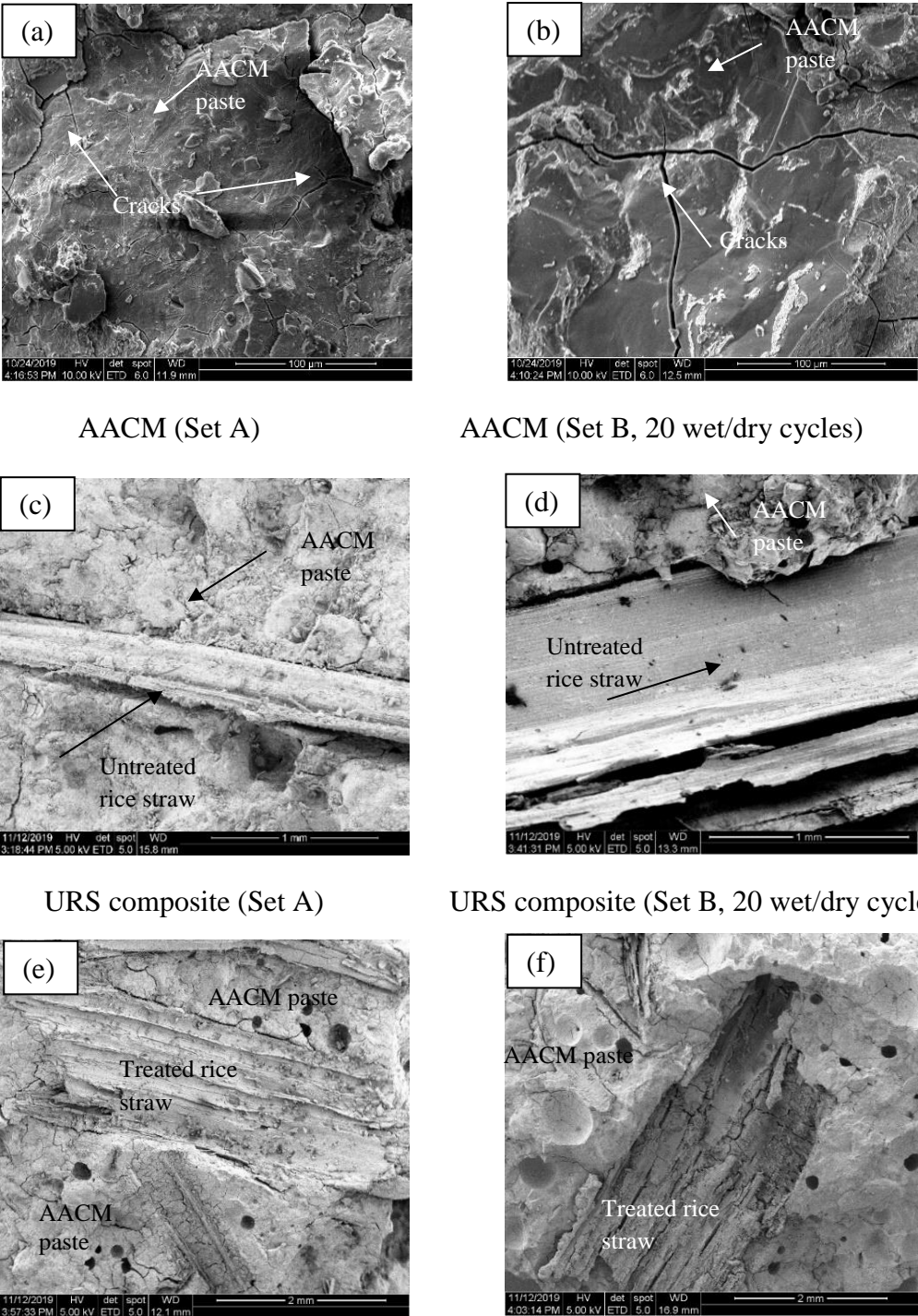


**Fig. 17.** SEMs of specimens of set A (reference) and set B (20 wet/dry cycles)

## 4. Conclusions

The main conclusions from the results reported in this paper are as follows:

- Alkali treatment with NaOH is an efficient method for enhancing the roughness of rice straw surface leading to an improvement of bond between the rice straw fibres and the alkali activated cementitious matrix.
- Both the untreated (URS) and treated (TRS) rice straw fibres with alkali reduce the workability of alkali activated cementitious composites (AACC). The reduction in workability of rice straw composites can be due to water absorption by the hydrophilic rice straw fibres. The TRS fibres resulted in a higher reduction in workability than the URS fibres since the TRS has higher dry surface areas than the URS fibres.
- The URS fibres reduce the flexural strength while TRS fibres increase the flexural strength in comparison with the control sample. The better performance of TRS fibre composite compared with the URS can be explained by the improvement of bond at the interface with the matrix due to the increase in effective surface area and surface roughness.
- Both the URS and TRS reinforcement improve the compressive strengths at 28 days compared with the control. This is due to the hydrophilic nature of rice straw leading to reduction in the liquid activator/binder ratio. In addition, the liquid absorbed in the rice straw fibres provides an internal curing agent enhancing the strength of AACM matrix. The maximum increase of 73% in compressive strength compared with the control occurs at 3% TRS at 28 days.
- Both URS and TRS reduce the water absorption of alkali activated cementitious composites. This may due to the reduction in bleeding as fibres increase mix stiffness and reduce the settlement of aggregates (sand). Greater volume of rice straw fibres leads to less water absorption. The largest reduction in water absorption is up to 60% compared with the control at 3% volume of the URS fibres.
- Both URS and TRS fibres reduce the drying shrinkage of AACC. The rice straw reduces the porosity of alkali activated cementitious composites because of the reduction in liquid activator/binder ratio caused by the hydrophilic nature of rice straw and the internal curing provided by the moisture held in the straw. The reduction in porosity and the moisture trapped in the fibres reduces shrinkage. At 90 days the 2% URS composite reduced the drying shrinkage by more than 40% compared with the control.
- In general, 1% and 2% of both URS and TRS fibres improve the durability of AACCs under wet/dry cycling as it increases the retained flexural strength ratios of the AACCs (between 0.62 and 0.69) compared to the control (0.55). In addition, 1% and 2% of both URS and TRS fibre reduces insignificantly the retained compressive strength ratios of the AACCs (between 0.9 and 1.06) compared to the control (1.09). The highest retained flexural strength ratio is found at 2% URS composites.
- Further research on the effect of different sources, lengths, treatment methods of rice straw on the mechanical properties including interfacial bond to the matrix is needed as these parameters are expected to contribute significantly to the properties of AACC.
- Further research is needed to analyse the functional groups of straw cellulose and the binding phases within the hardened matrix of the straw composites.

**Acknowledgments:** The authors would like to express their gratitude for National Foundation for Science and Technology Development of Vietnam (No.07/QD-HDQL-NAFOSTED) within The National Foundation for Science and Technology Development (NAFOSTED) – The UK Academies collaboration programme. The authors also gratefully acknowledge the support of the Materials and Engineering Research Institute, Sheffield Hallam University, UK and The University of Danang- University of Science and Technology, Vietnam.

**Funding:** This work was supported by the National Foundation for Science and Technology Development of Vietnam (No.07/QD-HDQL-NAFOSTED) within The National Foundation for Science and Technology Development (NAFOSTED) – The UK Academies collaboration programme. Funding was also contributed by the Materials and Engineering Research Institute, Sheffield Hallam University, UK to host the visiting researcher and support the experimental research.

**Author contributions:** **Chinh Van Nguyen:** Methodology, Data curation, Formal analysis, , Investigation, Validation, Funding acquisition, Roles/Writing - original draft; **P.S. Mangat:** Conceptualization, Resources, Supervision, Writing - review & editing.

## References

- [1] H. Stripple, C. Ljungkrantz, T. Gustafsson, R. Andersson, ‘CO<sub>2</sub> uptake in cement containing products- Background and calculation models for IPCC implementation, Report number: B 2309, IVL Swedish Environmental Research Institute Ltd (2018), <https://cembureau.eu/media/1753/ivl-report-co2-uptake-in-cement-containing-products-isbn-number-b2309.pdf>
- [2] C. Shi, P. Krivenko, D. Roy, Alkali- Activated Cements and Concretes, Taylor & Francis Group, 2005, ISBN 9780415700047 - CAT# RU0043X
- [3] P. Mangat, P. Lambert, Sustainability of alkali-activated cementitious materials and geopolymers, in: Sustain. Constr. Mater., Elsevier Ltd (2016) 459–476, [10.1016/B978-0-08-100370-1.00018-4](https://doi.org/10.1016/B978-0-08-100370-1.00018-4).
- [4] J.L. Provis, J.S.J. van Deventer, Alkali-Activated Materials State-of-the-Art Report, RILEM TC 224-AAM, 2014, DOI: [10.1007/978-94-007-7672-2](https://doi.org/10.1007/978-94-007-7672-2)
- [5] P. Duxson, J.L. Provis, Designing precursors for geopolymer cements, Journal of the American Ceramic Society 91 (2008) 3864–3869, <https://doi.org/10.1111/j.1551-2916.2008.02787.x>
- [6] B. Talling, P.V Krivenko, Blast furnace slag—the ultimate binder. In: Chandra, S. (Ed.), Waste Materials Used in Concrete Manufacturing, Noyes Publications, Park Ridge, NJ (1996) 235–289, <https://doi.org/10.1016/B978-081551393-3.50008-9>
- [7] O.O. Ojedokun, P.S Mangat, Chloride diffusion in alkali activated concrete. In: Second International Conference on Concrete Sustainability, ICCS Madrid 16 September (2016).
- [8] C.V. Nguyen, P. S. Mangat, G. Jones, Effect of shrinkage reducing admixture on the strength and shrinkage of alkali activated cementitious mortar, IOP Conf. Series: Materials Science and Engineering 371 (2018) 012022 doi:[10.1088/1757-899X/371/1/012022](https://doi.org/10.1088/1757-899X/371/1/012022)
- [9] P.S. Mangat, O.O. Ojedokun, Influence of curing on pore properties and strength of alkali activated Mortars, Construction and Building Materials 188 (2018) 337–348, <https://doi.org/10.1016/j.conbuildmat.2018.07.180>
- [10] J. Davidovits, Geopolymer Chemistry and Applications. Institut Géopolymère, Saint- Quentin, France (2008), ISBN: 9782951482098 (4th ed.)
- [11] G. Rostovskaya, V. Ilyin, A. Blazhis, A. The service properties of the slag alkaline concretes. In: Ertl, Z. (Ed.), Proceedings of the International Conference on Alkali Activated Materials—Research, Production and Utilization, Prague, Czech Republic, Česká rozvojová agentura (2007) 593–610.
- [12] M. Ardanuy, J. Claramunt, R. Filho, Cellulosic fibre reinforced cement-based composites: a review of recent research, Constr. Build. Mater. 79 (2015) 115–128, <https://doi.org/10.1016/j.conbuildmat.2015.01.035>



- [13] F. Pacheco-Torgal, S. Jalali, Cementitious building materials reinforced with vegetable fibres: a review, *Constr. Build. Mater.* 25 (2011) 575–581, <https://doi.org/10.1016/j.conbuildmat.2010.07.024>
- [14] Z. Li, X. Wang, L. Wang, Properties of hemp fibre reinforced concrete composites, *Compos. Part A* 37 (2006) 497–505, <https://doi.org/10.1016/j.compositesa.2005.01.032>
- [15] S.V. Joshi, L.T. Drzal, A.K. Mohanty, S. Arora, Are natural fibres composites environmentally superior to glass fibre reinforced composites?, *Compos Part A* 5 (2004) 371–376, <https://doi.org/10.1016/j.compositesa.2003.09.016>
- [16] O. Onuaguluchi, N. Banthia, Plant-based natural fibre reinforced cement composites: A review, *Cement and Concrete Composites* 68 (2016) 96–108, <https://doi.org/10.1016/j.cemconcomp.2016.02.014>
- [17] F. Ataie, Influence of Rice Straw Fibers on Concrete Strength and Drying Shrinkage, *Sustainability* (2018) 2445; [doi:10.3390/su10072445](https://doi.org/10.3390/su10072445)
- [18] I.N.M. Mohamed, Properties of rice straw cementitious composite, PhD Thesis, Darmstadt University of Technology, Germany, 2011, <https://core.ac.uk/download/pdf/11681186.pdf>
- [19] J. Chen, E. M.A. Elbashiry, T.Yu, Y. Ren, Z.Guo, S.Liu, Research progress of wheat straw and rice straw cement-based building materials in China, *Magazine of Concrete Research* 70(2018) 84–95, <https://doi.org/10.1680/jmacr.17.00064>
- [20] S. Mishra, A.K. Mohanty, L.T. Drzal, M. Misra, G. Hinrichsen, A review on pineapple leaf fibers, sisal fibers and their biocomposites, *Macromol. Mater. Eng.* 289 (2004) 955–974. [doi:10.1002/mame.200400132](https://doi.org/10.1002/mame.200400132)
- [21] D. Sedan, C. Pagnoux, A. Smith, T. Chotard, Mechanical properties of hemp fibre reinforced cement: Influence of the fibre/matrix interaction, *J. Eur. Ceram. Soc.* 28 (2008) 183–192, <https://doi.org/10.1016/j.jeurceramsoc.2007.05.019>
- [22] R.D. T. Filho, F.A. Silva, E.M.R. Fairbairn, J.A. M. Filho, Durability of compression molded sisal fiber reinforced mortar laminates, *Constr. Build. Mater* 23 (2009) 2409–2420, <https://doi.org/10.1016/j.conbuildmat.2008.10.012>
- [23] BS EN1015-3:1999, Methods of test for mortar for masonry- Part 3: Determination of consistence of fresh mortar (by flow table), BSi British Standard (1999)
- [24] BS EN1015-10:1999, Methods of test for mortar for masonry- Part 10: Determination of dry bulk density of hardened mortar, BSi British Standard (1999)
- [25] BS EN 196-1:2005, Method of testing cement- Part 1 Determination of strength- Compressive strength, BSi British Standard (2005)
- [26] ASTM C1403-15, Standard Test Method for Rate of Water Absorption of Masonry Mortars, ASTM Int. West Conshohocken, PA, 2015
- [27] ASTM C596-18, Standard Test Method for Drying Shrinkage of Mortar Containing Hydraulic Cement, West Conshohocken, PA, 2015
- [28] M. Troedec, D. Sedan, C. Peyratout, J. Bonneta, A. Smith, R. Guinebretiereb, V. Gloaguenc, P. Krausz, Influence of various chemical treatments on the composition and structure of hemp fibres, *Compos. Part A* 39 (2008) 514–522, <https://doi.org/10.1016/j.compositesa.2007.12.001>
- [29] L. Segal, C.M. Conrad, The characterization of cellulose derivatives using x-ray diffractometry, *American Dyestuff Reporter* (1957) 637–642.
- [30] L. Segal, J.J. Creely, A.E. Martin, C.M. Conrad, An empirical method for estimating the degree of crystallinity of native cellulose using the X-ray diffractometer, *Text. Resear. J* 29 (1959) 764–786.
- [31] M.A. Mansur, M.A. Aziz, A study on jute fibre reinforced cement composites, *Int J Cem Compos. Lightweight Concr.* 4 (2) (1982) 75–82, [https://doi.org/10.1016/0262-5075\(82\)90011-2](https://doi.org/10.1016/0262-5075(82)90011-2)
- [32] H. Savastano, V. Agopyan, A.M. Nolasco, L. Pimentel, Plant fibre reinforced cement components for roofing, *Constr. Build. Mater.* 13 (1999) 433–438, [https://doi.org/10.1016/S0950-0618\(99\)00046-X](https://doi.org/10.1016/S0950-0618(99)00046-X)
- [33] H.V. Le, D. Moon, D.J. Kim, Effects of ageing and storage conditions on the interfacial bond strength of steel fibers in mortars, *Construction and Building Materials* 170 (2018) 129–141, <https://doi.org/10.1016/j.conbuildmat.2018.03.064>
- [34] R.J. Gray, C.D. Johnston, The effect of matrix composition on fiber/matrix interfacial bond shear strength in fiber-reinforced mortar, *Cem. Concr. Res.* 14 (1984) 285–296, [https://doi.org/10.1016/0008-8846\(84\)90116-9](https://doi.org/10.1016/0008-8846(84)90116-9)

- [35] Y.W. Chan, V.C Li, Age effect on the characteristics of fibre-cement interfacial properties, *J. Mater. Sci.* 32 (1997) 5287–5292, <https://doi.org/10.1023/A:1018658626152>
- [36] D.J. Kim, S. El-Tawil, A. Naaman, Effect of matrix strength on pullout behaviour of high-strength deformed steel fibers, *ACI Spec. Publ.* (2010) 135–150.
- [37] T. Abu-Lebdeh, S. Hamoush, W. Heard, B. Zornig, Effect of matrix strength on pullout behavior of steel fiber reinforced very-high strength concrete composites, *Constr. Build. Mater.* 25 (2011) 39–46, <https://doi.org/10.1016/j.conbuildmat.2010.06.059>.
- [38] A.E. Naaman, H. Najm, Bond-slip mechanisms of steel fibers in concrete, *ACI Mater. J.* 88 (1991) 135–145.
- [39] J. Browning, D. Darwin, D. Reynolds, B. Pendergrass, Lightweight aggregate as internal curing agent to limit concrete shrinkage, *ACI Materials Journal*. 108 (2011) 638–644, <https://www.concrete.org/publications/internationalconcreteabstractsportal/m/details/id/51683467>
- [40] L.Q.N. Tran, C.A. Fuentes, C. Dupont-Gillain, Understanding the interfacial compatibility and adhesion of natural coir fibre thermoplastic composites, *Compos. Sci. Tech* 80 (2013) 23–30, [doi: 10.1016/j.compscitech.2013.03.004](https://doi.org/10.1016/j.compscitech.2013.03.004)
- [41] B.L.S. Sipião, L.S. Reis, R.D.L.M. Paiva, M.R. Capri, D.R. Mulinari, Interfacial adhesion in natural fiber-reinforced polymer composites. In *Lignocellulosic Polymer Composites: Processing, Characterization and Properties*; Wiley: New York, USA (2014) 17–39, <https://doi.org/10.1002/9781118773949.ch2>
- [42] M. Hao, H. Wu, F. Qiu, X. Wang, Interface bond improvement of sisal fibre reinforced polylactide composites with added epoxy oligomer, *Materials* 11 (2018) 398, [doi:10.3390/ma11030398](https://doi.org/10.3390/ma11030398)
- [43] N. Sgriccia, M.C. Hawley, M. Misra, Characterization of natural fiber surfaces and natural fiber composites, *Compos. Part A Appl. Sci. Manuf* 39 (2008) 1632–1637, <https://doi.org/10.1016/j.compositesa.2008.07.007>
- [44] G.N. Farahani, I. Ahmad, Z. Mosadeghzad, Effect of fiber content, fiber length and alkali treatment on properties of kenaf fiber/UPR composites based on recycled PET wastes, *Polym. Plast. Technol. Eng* 51(2012) 634–639, <https://doi.org/10.1080/03602559.2012.659314>
- [45] B.L.S. Sipião, L.S. Reis, R.D.L.M. Paiva, M.R. Capri, D.R. Mulinari, Chemical modification and properties of cellulose-based polymer composites. In *Lignocellulosic Polymer Composites: Processing, Characterization and Properties*; Wiley: New York, USA (2014) 301–323, <https://doi.org/10.1002/9781118773949.ch14>
- [46] N. Banthia, A. Bhargava, Permeability of stressed concrete and role of fiber reinforcement, *ACI Mater J.* 104 (1) (2007) 70–76.
- [47] Y. Xu, D.D.L. Chung, Reducing the drying shrinkage of cement paste by admixture surface treatments, *Cement and Concrete Research* 30 (2000) 241–245, [https://doi.org/10.1016/S00088846\(99\)00239-2](https://doi.org/10.1016/S00088846(99)00239-2)
- [48] P. S. Mangat, M.M. Azari, Shrinkage of steel fibre reinforced cement composites, *Materials and Structures* 21 (1988), 163–171, <https://doi.org/10.1007/BF02473051>
- [49] E.T. Dawood, M. Ramli, High strength characteristics of cement mortar reinforced with hybrid fibres, *Construction and Building Materials* 25 (2011) 2240–2247, <https://doi.org/10.1016/j.conbuildmat.2010.11.008>
- [50] R.D. Toledo Filho, K. Ghavami, M.A. Sanjuan, G.L. England, Free, restrained and drying shrinkage of cement mortar composites reinforced with vegetable fibres, *Cem. Concr. Compos.* 27 (2005) 537e546, <https://doi.org/10.1016/j.cemconcomp.2004.09.005>
- [51] J. F.A. Silva, R.D. Toledo Filho, J.A. Melo Filho, E.M.R. Fairbairn, Physical and mechanical properties of durable sisal fibre-cement composites, *Constr. Build. Mater* 24 (2010) 777–785, <https://doi.org/10.1016/j.conbuildmat.2009.10.030>.
- [52] B.J. Mohr, H. Nanko, K.E. Kurtis, Durability of kraft pulp fiber-cement composites to wet/dry cycling, *Cement & Concrete Composites* 27 (2005) 435–448, <https://doi.org/10.1016/j.cemconcomp.2004.07.006>